

# Photonic Generation of Microwave Waveforms Based on a Polarization Modulator in a Sagnac Loop

Weilin Liu, *Student Member, IEEE*, and Jianping Yao, *Fellow, IEEE, Fellow, OSA*

**Abstract**—An optical microwave waveform generator using a polarization modulator (PolM) in a Sagnac loop is proposed and experimentally demonstrated. Microwave waveforms including a triangular waveform, a sawtooth waveform, and a square waveform, can be generated using a sinusoidal signal to modulate a light wave at a PolM in a Sagnac loop. In the proposed microwave waveform generator, a sinusoidal microwave signal is applied to the PolM in the Sagnac loop. Due to the velocity mismatch, only the clockwise light wave in the Sagnac loop is effectively modulated by the sinusoidal microwave signal at the PolM, and the counter-clockwise light wave is not modulated. Along the clockwise direction, the powers of the odd- and even-order sidebands can be controlled separately by tuning a polarization controller after the PolM. In addition, the output power of the optical carrier can be independently controlled by combining the counter-clockwise and clockwise optical carriers at the output of a polarization beam splitter. As a result, a modulated signal with controllable odd- and even-order sidebands is generated. By applying the modulated signal to a photodetector, a microwave signal with fully controllable odd- and even-order harmonics is generated, which corresponds to a desired microwave waveform. A theoretical analysis is developed, which is validated by an experiment. A triangular, sawtooth, and square waveform with a repetition rate tunable from 2 to 4 GHz is experimentally generated.

**Index Terms**—Carrier suppression, microwave photonics, microwave technology, optical interference, optical polarization, photonic generation of microwave signals, polarization modulation.

## I. INTRODUCTION

PHOTONICS generation of arbitrary microwave waveforms has been a topic of interest recently, which can find many important applications in modern radar systems [1], wired and wireless communications [2], [3], and all-optical microwave signal processing and manipulation [4], [5]. Various optical approaches have been reported to generate microwave waveforms. Microwave waveforms can be generated based on optical spectral shaping [6], [7]. In the approach, an optical pulse train generated by an optical comb generator or a mode locked laser (MLL) serving as a coherent broadband source is sent to an

optical spectral shaper, which tailors the input spectrum such that a desired microwave waveform is generated by applying the tailored optical pulse train to a photodetector (PD). In [6], an optical spectral shaper based on a liquid crystal modulator (LCM) was employed to line-by-line control the magnitude and phase of each of the comb lines to make the entire spectrum identical to that of a triangular waveform. The system can be extended to generate arbitrary waveforms by controlling the LCM with different magnitude and phase response. Recently, a technique to generate arbitrary waveforms based on frequency-to-time mapping was proposed [7]. In the demonstration in [7], two cascaded filters working as an optical spectral shaper were employed to shape an ultra-short optical pulse to have a spectrum with a triangular shape. Through frequency-to-time mapping in a dispersive element, a triangular pulse was generated. To generate different waveforms, different optical filters have to be used, which limits the system flexibility.

A microwave waveform can also be generated through pulse shaping in a nonlinear and normally-dispersive fiber. For example, in [8] a transform-limited pulse train generated by an MLL was sent through a pre-chirping fiber and an erbium-doped fiber amplifier (EDFA). By choosing the length of the fiber and tuning the pulse power at the output of the EDFA, a triangular pulse train is generated after progressive pulse reshaping in a nonlinear and normally-dispersive fiber. The major limitation of the technique is that the desired dispersion and nonlinearity were difficult to manipulate for real applications.

Furthermore, a microwave waveform can be generated by manipulating electro-optical modulation harmonics. In [9], a continuous-wave (CW) light wave was modulated by a reference radio-frequency (RF) signal through a dual-electrode Mach-Zehnder modulator (De-MZM). By controlling the bias voltage to the De-MZM, even-order sidebands were suppressed. The remaining odd-order sidebands were further manipulated in their phase terms by a length of dispersive fiber. A triangular waveform was thus generated at a high-speed PD. The repetition rate of the generated triangular waveform is two times the frequency of the reference RF signal. This approach is simple and cost effective, but the repetition rate is difficult to tune because the dispersion value needed in the system is dependent on the frequency and the power of the reference RF signal.

In addition to the above techniques in [6]–[9], microwave waveforms can also be generated based on temporal Talbot effect [10], [11], using a microwave photonic filter [12], [13], and based on temporal pulse shaping [14]. The major limitation of these techniques in [10]–[14] is that the repetition rate of the generated waveform is difficult to tune, which limits the applications where a tunable repetition rate is needed.

Manuscript received December 29, 2013; revised February 24, 2014 and March 16, 2014; accepted March 18, 2014. Date of publication March 19, 2014; date of current version September 1, 2014. This work was supported by the Natural Science and Engineering Research Council of Canada.

The authors are with the Microwave Photonics Research Laboratory, School of Electrical Engineering and Computer Science, University of Ottawa, ON K1N 6N5, Canada (e-mail: jpyao@eecs.uOttawa.ca).

Color versions of one or more of the figures in this paper are available online at <http://ieeexplore.ieee.org>.

Digital Object Identifier 10.1109/JLT.2014.2312819

Recently, we proposed a novel approach to generating a triangular waveform sequence with a tunable repetition rate using a single polarization modulator (PolM) in a Sagnac loop [15]. The fundamental concept of the approach is to manipulate the spectrum of an optical signal to be identical to that of a triangular waveform. It is known that a triangular waveform sequence has a Fourier series with only odd-order harmonics, which can be realized using a sinusoidal signal to modulate a light wave at a PolM in a Sagnac loop. In the proposed waveform generator, a sinusoidal microwave signal is applied to the PolM. Due to the velocity mismatch, only the clockwise light wave in the Sagnac loop is effectively modulated and the counter-clockwise light wave is not. Along the clockwise direction, the even-order sidebands are suppressed by tuning a polarization controller (PC) after the PolM. As a result, a modulated signal with only the odd-order sidebands is generated, which is combined with the counter-clockwise propagated optical carrier at the output of a polarization beam splitter (PBS). By applying the combined signal to a PD, a microwave signal with only the odd-order harmonics is generated, which corresponds to a triangular waveform.

The approach reported in [15] can be extended to generate other types of microwave waveforms with a tunable repetition rate. In this paper, we provide a detailed theoretical as well as experimental study of the technique for the generation of microwave waveforms reported in [15]. By manipulating the system parameters, such as the input RF power level and the polarization states at different locations in the system, the generator can be reconfigured to generate other types of microwave waveforms. The approach is evaluated by simulations which are then verified by experiments. The generation of a triangular, sawtooth, and square waveform with a repetition rate tunable from 2 to 4 GHz is experimentally demonstrated.

The paper is organized as follows. In Section II, the principle of the proposed approach is presented, with an emphasis on the accurate manipulation of the electro-optical modulation sidebands through controlling the system parameters, such as the input RF power and the polarization states at different locations in the system. Numerical simulations are then performed. In Section III, an experimental demonstration is presented. A triangular waveform, a sawtooth waveform, and a square waveform with a tunable repetition rate from 2 to 4 GHz are generated. A conclusion is drawn in Section IV.

## II. PRINCIPLE

Fig. 1 shows the schematic of the proposed microwave waveform generator. A linearly polarized CW light wave from a tunable laser source (TLS) is sent to a Sagnac loop through a PBS, to split the input light wave into two orthogonally polarized light waves to travel along the clockwise and counter-clockwise directions in the Sagnac loop, in which a PolM is incorporated. A PC (PC1) after the TLS is used to align the polarization direction of the light wave from the TLS to have an angle relative to one principal axis of the PBS. As can be seen from Fig. 1, the two linearly polarized clockwise and counter-clockwise light waves are incident into the PolM from the opposite directions. Along

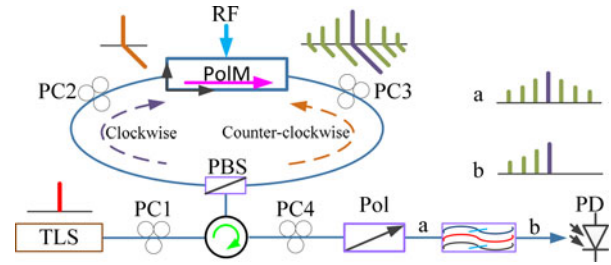


Fig. 1. Schematic of the proposed microwave waveform generator. TLS: tunable laser source; PC: polarization control; PBS: polarization beam splitter; RF: radio frequency; PolM: polarization modulator; Pol: polarizer; PD: photodetector.

the clockwise direction, the light wave and the microwave are traveling in the same direction. Since the PolM is designed to match the velocities of the light wave and the microwave [16], a strong modulation is obtained. Along the counter-clockwise direction, however, the light wave and the microwave are traveling in the opposite directions, since the light wave and the microwave only meet at a very short time, very weak modulation will be produced. Therefore, only the clockwise light wave is effectively modulated by a reference microwave signal at the PolM, and the counter-clockwise light wave is not modulated. As a result, a modulated and a non-modulated optical signal with opposite propagation directions are obtained. Notice that along the clockwise direction, the PolM in conjunction with a PC (PC2) and the PBS operates as an equivalent MZM with the bias point controlled by a tunable static phase shift introduced by PC3 [17], [18]. Thus, the modulated optical signal is combined with the counter-clockwise propagated optical carrier at a polarizer. By applying an optical bandpass filter to remove the negative order sidebands, and apply the positive order sidebands including the optical carrier to a PD, a microwave waveform is generated.

$$E_{\text{PBS-cw}} = \frac{E_{\text{cw}}}{2} \exp(j\omega t) \left\{ [1 + \exp(j\varphi)] J_0(\beta) + \sum_{k=1}^{\infty} [(-1)^k + \exp(j\varphi)] J_k(\beta) [(-1)^k \exp(jk\omega_m t) + \exp(-jk\omega_m t)] \right\}. \quad (1)$$

As shown in Fig. 1, along the clockwise direction, the joint operation of the PolM, PC3, and the PBS corresponds to an MZM with the bias point controlled by PC3 to introduce a static phase shift. In this way, the amplitude of the harmonics can be tuned. Assuming that the amplitude of the electrical field of the CW light wave from the TLS is  $E_0$ , and the polarization direction of the incident light from the TLS is aligned at an angle of  $\theta$  relative to one principal axis of the PBS, the electrical field at the output of the PBS for the clockwise propagation light wave can be expressed in (1) at the bottom of the page, where  $E_{\text{cw}} = E_0 \cos \theta$  is the amplitude of the electrical field of the clockwise propagation light wave,  $\beta$  is the phase modulation index,  $\omega$  and  $\omega_m$  are the angular frequencies of the optical carrier and the microwave signal, respectively,  $\varphi$  is a static phase term introduced by PC3 placed between the PolM and the PBS.

Combining the counter-clockwise non-modulated optical signal with the clockwise optical signal at the polarizer, and assuming that the principal axis of the polarizer is aligned at an angle of  $\alpha$  to one principal axis of the PBS, the electrical field at the output of the polarizer can be expressed as

$$E_{\text{pol}} = E_{\text{PBS-cw}} \cos \alpha + E_{\text{PBS-ccw}} \sin \alpha \quad (2)$$

where  $E_{\text{PBS-ccw}} = E_0 \exp(j\omega t) \sin \theta$  is the electrical field of the counter-clockwise light wave at the output of the PBS. Notice that the negative and positive odd-order sidebands are out of phase when the even-order sidebands are suppressed, an optical bandpass filter is required to remove the negative order sidebands (or positive order sidebands) for generating waveforms with only odd-order harmonics. Thus, the electrical field after the optical bandpass filter is given by

$$E_{\text{out}} = E_0 \exp(j\omega t) \times \left\{ A + \frac{1}{2} B \sum_{k=0}^{\infty} [1 + \exp(j\varphi + jk\pi)] J_k(\beta) \exp(jk\omega_m t) \right\} \quad (3)$$

where  $A = \sin \alpha \sin \theta$  and  $B = \cos \alpha \cos \theta$ . By applying the signal at the output of the optical bandpass filter to the high speed PD, we have an electrical signal at the output of the PD, given by

$$I(t) = R \cdot E_{\text{out}} \cdot E_{\text{out}}^* \approx I_{\text{dc}} + C_{e.o.} \sum_{k=1}^{\infty} J_k(\beta) \cos\left(k\frac{\pi}{2} + \frac{\varphi}{2}\right) \cos\left(k\omega_m t + k\frac{\pi}{2} - \varphi_c\right) \quad (4)$$

where  $R$  is the responsivity of the PD,  $C_{e.o.}$  is a constant, and  $\varphi_c$  is a static phase term given by

$$\varphi_c = \arcsin \frac{A \sin \frac{\varphi}{2}}{\sqrt{A^2 \sin^2 \frac{\varphi}{2} + \cos^2 \frac{\varphi}{2} [A + B J_0(\beta)]^2}}$$

### A. Triangular Waveform

The Fourier series expansion of a typical triangular waveform sequence  $T_t(t)$  is given by

$$T_{\text{tr}}(t) = C_{\text{tr}} + D_{\text{tr}} \sum_{k=1,3,5}^{\infty} \frac{1}{k^2} \cos k\Omega t \quad (5)$$

where  $C_{\text{tr}}$  and  $D_{\text{tr}}$  are two constants, and  $\Omega$  is the fundamental angular frequency. As can be seen from (5), a triangular waveform has only odd-order harmonics. To obtain an electrical signal with a spectrum containing the odd-order harmonics, the even-order harmonics need to be suppressed, which can be realized by biasing the equivalent MZM at the minimum transmission point (MITP) or equivalently to let  $\varphi = \pi$ , as shown in (4). Comparing the expression of  $I(t)$  in (4) with the Fourier series expansion of a typical triangular waveform sequence  $T_{\text{tr}}(t)$  in (5), to generate an ideal triangular waveform, and assuming that  $\theta = \alpha = \pi/4$ , we should have

$$\frac{J_k(\beta)}{J_1(\beta)} = \frac{1}{k^2} \quad (6)$$

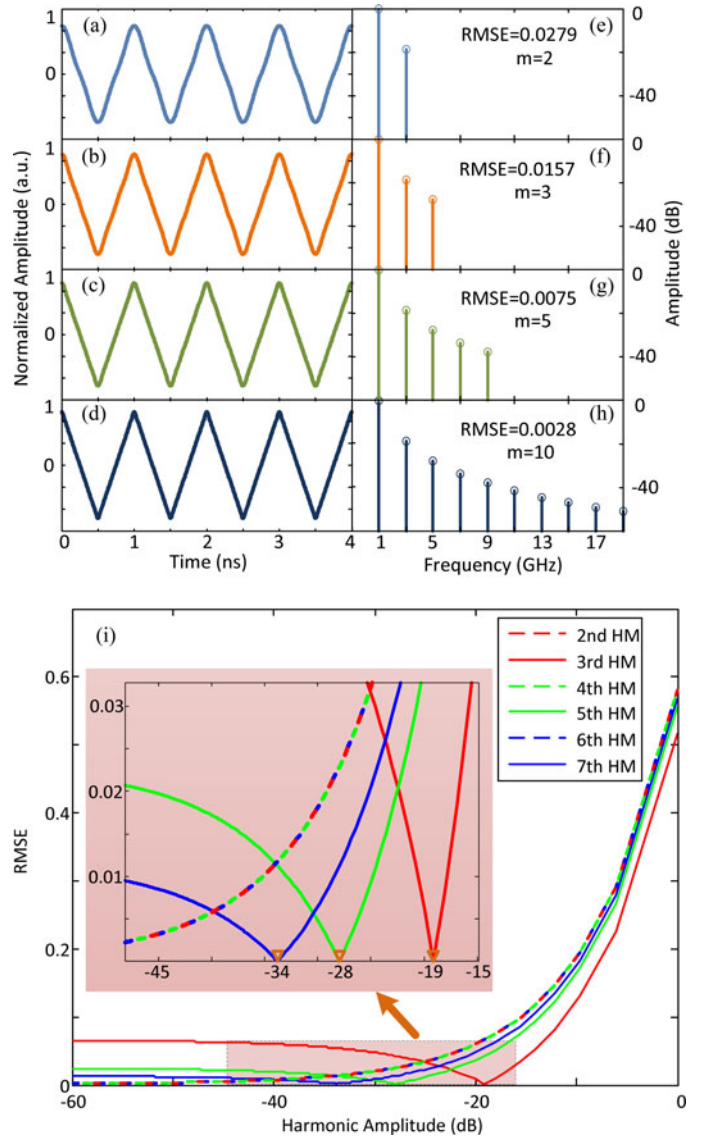


Fig. 2. Simulation results. Reconstructed temporal triangular waveform sequence with the number of Fourier series components of (a) 2, (b) 3, (c) 5, and (d) 10. The amplitudes of the corresponding Fourier series components are shown in (e), (f), (g) and (h). (i) Error analysis at different harmonic power levels for seven harmonics, each of which is calculated when the other harmonics are at the ideal power levels. The RMSE curves for the even-order harmonics at 2, 4 and 6 are overlapped, as shown in the dashed lines, which indicates that the even-order harmonics contribute an identical RMSE at the same power level. RMSE: root mean square error; HM: harmonic.

where  $k = 3, 5, 7, \dots$  is the order of the Bessel function of the first kind. For a given phase modulation index  $\beta$ , (6) cannot be satisfied for every  $k$ , an ideal triangular-shaped waveform is not feasible. However, a triangular waveform can be approximated by a finite number of the Fourier series components. We perform a simulation to evaluate the errors between an ideal triangular waveform and a triangular waveform with a finite number of Fourier series components, with the results shown in Fig. 2(a) to (h), where  $m$  is the number of Fourier series components. The root-mean square errors (RMSEs) corresponding to different number of Fourier series components are also shown. As can be seen, two Fourier components can provide a good

approximation of a triangular waveform. Since the powers of the high order Fourier components are dropping fast, as shown in (5), even no visible difference between triangular waveforms reconstructed using five and ten Fourier series components. In our experimental demonstration, two Fourier components will be considered, and (6) can be rewritten as

$$\frac{J_3(\beta)}{J_1(\beta)} = \frac{1}{9} \quad (7)$$

which can be realized if the modulation index is controlled to be

$$\beta = 1.51 \quad (8)$$

which can be realized by controlling the power level of the modulation microwave signal.

In a real system, the even-order harmonics may not be completely suppressed, and the 3rd harmonic is difficult to maintain a fixed power level for different frequencies without power adjustment. Thus, the change of the power level of each harmonic to the accuracy of the generated triangular waveform is evaluated. As shown in Fig. 2(i), the insufficiently suppression of the even-order harmonics would lead to a large RMSE, and the power level of each odd-harmonic can be chosen to have a minimum RMSE, which is marked with a small triangle in Fig. 2(i). To generate a high accuracy triangular waveform, the even-order harmonics should be fully suppressed. In addition, the power level of each odd-order harmonic should be controlled identical to the ideal value to ensure the generation of an accurate triangular waveform. Practically, to generate a good triangular waveform, the even-order harmonics should be suppressed by 30 dB, and the power levels of the odd-order harmonics should be maintained close to the marked values in Fig. 2(i).

### B. Sawtooth Waveform

The Fourier series expansion of a typical sawtooth waveform sequence  $T_s(t)$  is given by

$$T_{sa}(t) = C_{sa} + D_{sa} \sum_{k=1}^{\infty} \frac{1}{k} \sin(k\Omega t) \quad (9)$$

where  $C_{sa}$  and  $D_{sa}$  are two constants. As can be seen from (9), a sawtooth waveform has both odd- and even-order harmonics. Comparing the expression of  $I(t)$  in (4) with the Fourier series expansion of a sawtooth waveform sequence  $T_{sa}(t)$  in (9), to generate an ideal sawtooth waveform, we should have

$$\begin{cases} \frac{J_k(\beta) \cos(k\frac{\pi}{2} + \frac{\varphi}{2})}{J_1(\beta) \cos(\frac{\pi}{2} + \frac{\varphi}{2})} = \frac{1}{k} \\ \varphi_c = \frac{\pi}{2} \end{cases} \quad (10)$$

where  $k = 2, 3, 4, \dots$  is the order of the Bessel function of the first kind. For a given phase modulation index  $\beta$ , (12) cannot be satisfied for every  $k$ , thus an ideal sawtooth-shaped waveform cannot be generated. However, if we only consider a finite number of Fourier series components, a sawtooth waveform can also be approximated. As shown in Fig. 3, a limited number of the Fourier series components can provide a good approximation of

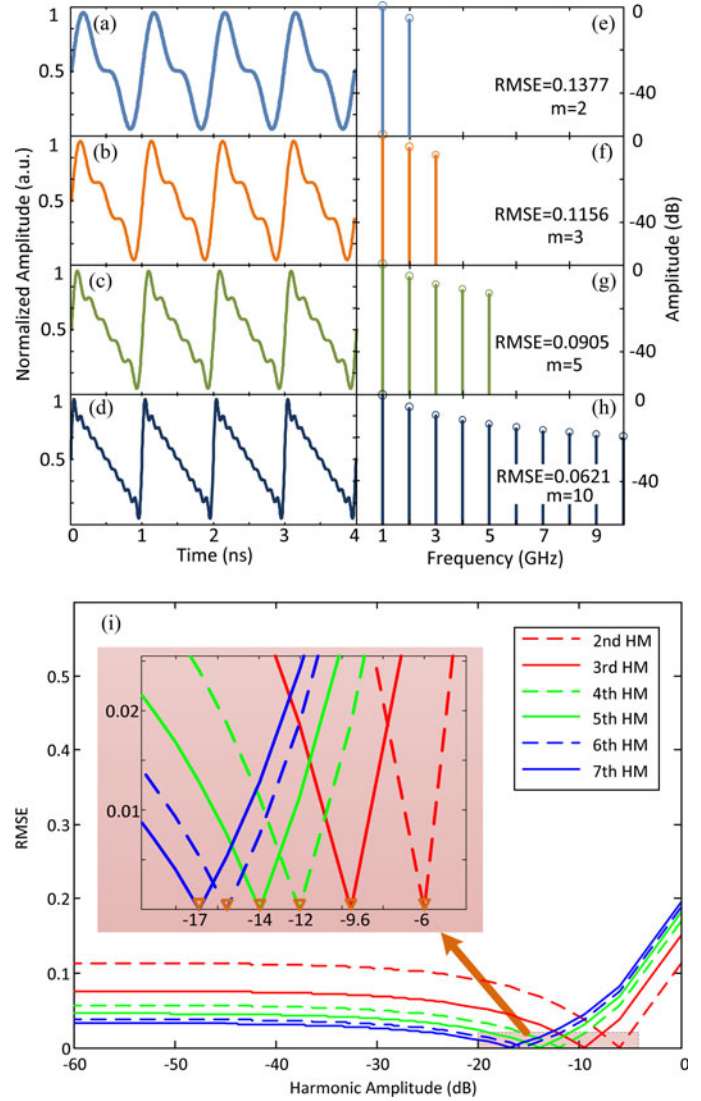


Fig. 3. Simulation results. Reconstructed temporal sawtooth waveform sequence with the number of Fourier series components of (a) 2, (b) 3, (c) 5, and (d) 10. The amplitudes of the corresponding Fourier series components are shown in (e), (f), (g) and (h). (i) Error analysis at different harmonic power levels for seven harmonics, each of which is calculated when the other harmonics are at the ideal power levels.

a sawtooth waveform. When two series components are used, the RMSE is 0.1377, and when three Fourier series components are used, the RMSE is as small as 0.1156. In our experimental demonstration, three Fourier series components are used, thus (12) is simplified to

$$\begin{cases} \frac{J_2(\beta)}{J_1(\beta)} = \frac{\sin(\frac{\varphi}{2})}{2 \cos(\frac{\varphi}{2})} \\ \frac{J_3(\beta)}{J_1(\beta)} = -\frac{1}{3} \end{cases} \quad (11)$$

which can be simply achieved if the static phase and the phase modulation index are given by

$$\begin{cases} \varphi = 0.35\pi \\ \beta = 6.10 \end{cases} \quad (12)$$

which can be implemented by tuning PC3 and the power of the microwave signal, respectively.

The effect of the power level of each harmonic on the accuracy of the generated sawtooth waveform is also discussed. As shown in Fig. 3(i), the power level of each harmonic can be chosen to have a minimum RMSE, which is marked with a small triangle in Fig. 3(i). To achieve the highest accuracy of the generated sawtooth waveform, the power levels of the harmonics should be maintained close to the marked values in Fig. 3(i)

### C. Square Waveform

The Fourier series expansion of a typical square waveform sequence  $T_{sq}(t)$  is given by

$$T_{sq}(t) = C_{sq} + D_{sq} \sum_{k=1,3,5}^{\infty} \frac{1}{k} \sin(k\Omega t) \quad (13)$$

where  $C_{sq}$  and  $D_{sq}$  are two constants. As can be seen from (13), a square waveform has only odd-order harmonics. Similar to the triangular waveform generation, to obtain an electrical signal with a spectrum containing the fundamental and the odd-order harmonics, the equivalent MZM should be biased at the MITP to make  $\varphi = (2l + 1)\pi$ ,  $l = 0, 1, 2, 3, \dots$ . Comparing the expression  $I(t)$  in (4) with the Fourier series expansion of a typical square waveform sequence  $T_{sq}(t)$  in (13), to generate an ideal square waveform, and assuming that  $\theta = \alpha = \pi/4$ , we should have

$$\frac{J_k(\beta)}{J_1(\beta)} = (-1)^{\frac{k-1}{2}} \frac{1}{k} \quad (14)$$

where  $k = 3, 5, 7, \dots$  is the order of the Bessel function. For a given phase modulation index  $\beta$ , (14) cannot be satisfied for every  $k$ , thus an ideal square waveform cannot be generated. Similar to the triangular waveform generation, a square waveform can be approximated by a finite number of Fourier series components. As shown in Fig. 4, a limited number of the Fourier series components can provide a good approximation of a square waveform. However, compared with the generation of a triangular waveform, the generation of a square waveform needs more Fourier series components to maintain the same level of RMSE. In our experimental demonstration, due to the limited input microwave power, two Fourier series components will be considered, and (14) is now given by

$$\frac{J_3(\beta)}{J_1(\beta)} = -\frac{1}{3} \quad (15)$$

which can be realized if the modulation index is

$$\beta = 6.10. \quad (16)$$

Similar to the triangular waveform generation, the effect of the power level of each harmonic on the accuracy of the generated

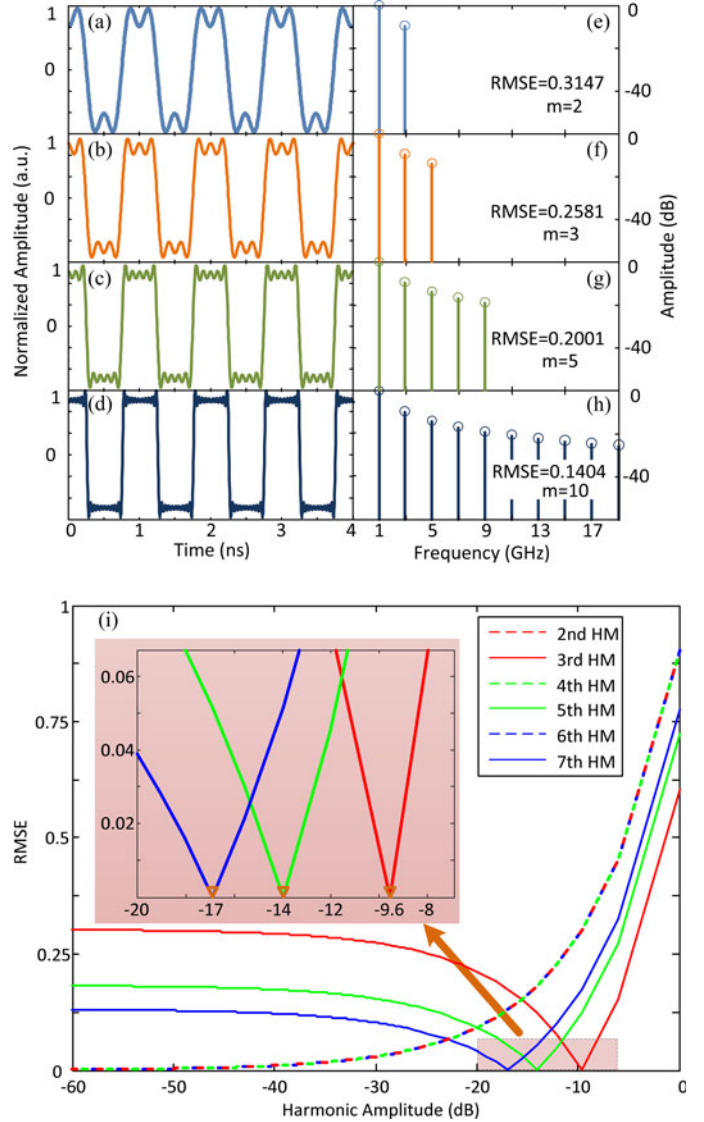


Fig. 4. Simulation results. Reconstructed temporal square waveform sequence with the number of Fourier series components of (a) 2, (b) 3, (c) 5, and (d) 10. The amplitudes of the corresponding Fourier series components are shown in (e), (f), (g) and (h). (i) Error analysis at different harmonic power levels for seven harmonics, each of which is calculated when the other harmonics are at the ideal power levels. The RMSE curves for the even-order harmonics are overlapped, as shown in the dashed lines, which indicates that the even-order harmonics contribute the same RMSE at a same power level.

square waveform is evaluated. As shown in Fig. 4(i), the insufficient suppression of the even-order harmonics would lead to a large RMSE, and the power level of each odd-harmonic can be chosen to have a minimum RMSE, which is marked with a small triangle in Fig. 4(i). In real applications, the power levels of the odd-order harmonics should be maintained close to the marked values in Fig. 4(i).

### D. Arbitrary Waveform

Now we discuss the use of the proposed approach to the generation of an arbitrary microwave waveform. The Fourier series expansion of an arbitrary waveform sequence  $T(t)$  is

given by

$$\begin{aligned} S(t) &= C + D \sum_{k=1}^{\infty} a_k \cos(k\Omega t) + b_k \sin(k\Omega t) \\ &= C + D \sum_{k=1}^{\infty} c_k \cos(k\Omega t + \varphi_k) \end{aligned} \quad (17)$$

where  $C$  and  $D$  are two constants. Comparing it with (4), we have

$$\begin{cases} \frac{J_k(\beta) \cos\left(k\frac{\pi}{2} + \frac{\varphi}{2}\right)}{J_1(\beta) \cos\left(\frac{\pi}{2} + \frac{\varphi}{2}\right)} = \frac{1}{k} \\ \varphi_k = \varphi_c \end{cases} \quad (18)$$

where  $k = 2, 3, 4, \dots$  is the order of the Bessel function of the first kind. If the static phase terms of all harmonic are identical, the proposed system can generate at least three harmonics which satisfy (18). For most waveforms, the fundamental, the second and third harmonics largely dominates the shape of the waveform. In this case, the propose system can approximately generate arbitrary waveforms if the static phase terms of all harmonics are identical.

### III. EXPERIMENT

A proof-of-concept experiment based on the setup shown in Fig. 1 is implemented. A linearly polarized CW light wave at 1550.37 nm from the TLS (N7714A, Agilent) is sent to the Sagnac loop through PC1 and the PBS. Two orthogonally polarized light waves travel along the opposite directions in the Sagnac loop and pass through the PolM (Versawave, 40-GHz polarization modulator). Due to the velocity mismatch, only the clockwise light wave is effectively modulated by the reference sinusoidal microwave signal applied to the PolM, and the counter-clockwise propagation light wave is not modulated. As a result, a modulated and a non-modulated optical signal with opposite propagation directions are obtained at the output of the PBS. By adjusting PC2 and PC3, the power levels of the sidebands are controlled at the output of the PBS. The non-modulated optical signal is combined with the modulated optical signal at the polarizer. After an optical bandpass filter (WaveShaper 4000 S, Finisar), an optical signal consisting of an optical carrier and sidebands with controllable power levels are obtained. By applying this optical signal to the PD, a desired microwave waveform, including a triangular waveform, a sawtooth waveform, and a square waveform, with a repetition rate identical to the reference sinusoidal microwave frequency is generated.

#### A. Triangular Waveform

In the experiment, a reference sinusoidal microwave signal with a tunable frequency from 2 to 4 GHz generated by a signal generator (Agilent E8254A) is applied to the PolM. Considering the half-wave voltage of the PolM is 3.3 V, the power of the microwave signal is controlled to be 14 dBm, corresponding to a modulation index of 1.51. By tuning PC2 and PC3, the second-order sidebands are suppressed. The non-modulated

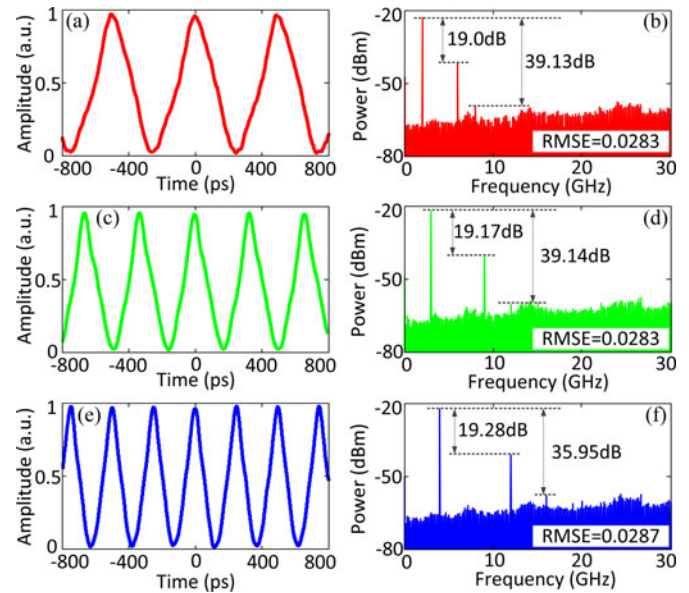


Fig. 5. Experiment results. (a) Generated triangular waveform with a repetition rate of 2 GHz, and (b) its spectrum. (c) Generated triangular waveform with a repetition rate of 3 GHz, and (d) its spectrum. (e) Generated triangular waveform with a repetition rate of 4 GHz, and (f) its spectrum.

optical signal is combined with the modulated signal, which contributes to the strong optical carrier. Since the positive- and negative-order sidebands are out of phase, the negative-order sidebands are removed by the optical filter to ensure effective signal generation. Thus, an optical signal with the first-, the third-order sidebands and the optical carrier is obtained.

By applying the optical signal to the high-speed PD (New Focus Model 1014, 25 GHz), a triangular waveform with a repetition rate identical to the frequency of the reference microwave signal is generated. The temporal waveform of the generated microwave signal is measured by a real-time oscilloscope (DSO, Agilent X93204A) and its spectrum is measured by an electrical spectrum analyzer (ESA, Agilent E4448A). When the microwave frequency is tuned at 2 GHz, a triangular waveform with a repetition rate of 2 GHz is generated, as shown in Fig. 5(a). The spectrum of the triangular waveform is shown in Fig. 5(b). To evaluate the repetition rate tunability, the microwave frequency is continuously increased from 2 to 4 GHz while maintaining the other parameters in the system (setting of PC1, PC2, PC3, and PC4, and input microwave power) unchanged, a triangular waveform with an increased repetition rate is generated. Fig. 5(c) and (e) shows the triangular waveforms at 3 and 4 GHz and the corresponding spectra are shown in Fig. 5(d) and (f). This important feature makes the generation of a widely repetition-rate-tunable triangular waveform greatly simplified. The RMSEs of the experimentally generated triangular waveforms are also calculated. For the triangular waveforms at 2, 3, and 4 GHz, the RMSEs are 0.0283, 0.0283, and 0.0287, respectively. The theoretical RMSE calculated in the simulation for the triangular waveform with two Fourier series components is 0.0279. It can be seen that the experimentally generated triangular waveforms match well with the simulated waveforms. The small deterioration of RMSE is due to the difference

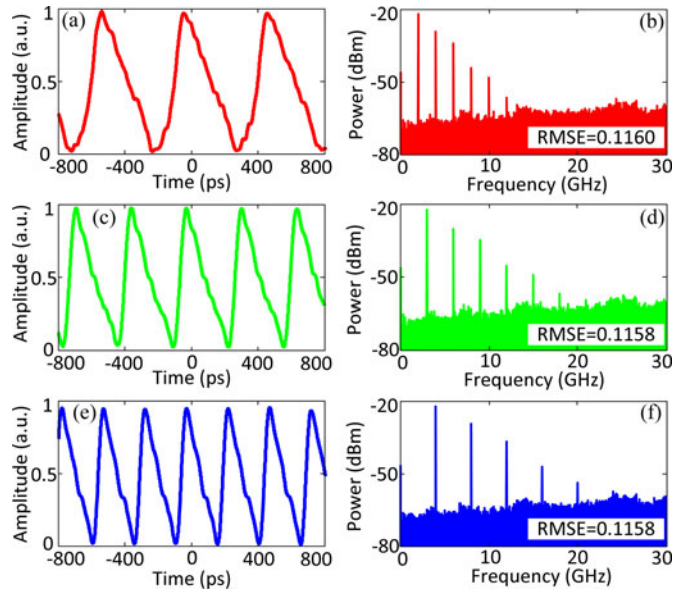


Fig. 6. Experiment results. (a) Generated sawtooth waveform with a repetition rate of 2 GHz, and (b) its spectrum. (c) Generated sawtooth waveform with a repetition rate of 3 GHz, and (d) its spectrum. (e) Generated sawtooth waveform with a repetition rate of 4 GHz, and (f) its spectrum.

between the theoretical and experimental power distributions of the Fourier series components. In the experiment, it is difficult to control the power levels of the individual spectral lines.

### B. Sawtooth Waveform

To generate a sawtooth waveform, the power of the microwave signal is controlled to be 26 dBm, corresponding to a modulation index of 6.10. By tuning PC2 and PC3, both the even- and odd-order sidebands are well controlled to ensure that the power levels of the generated microwave harmonics comply with (11), and by tuning PC1 and PC4, the static phase is controlled to be  $\varphi_c = \pi/2$ , as given in (10). By applying the optical signal to the high speed PD, a sawtooth waveform with a repetition rate identical to the frequency of the reference microwave signal is generated. In the experiment, when the microwave frequency is tuned at 2 GHz, a sawtooth waveform with a repetition rate of 2 GHz is generated, as shown in Fig. 6(a). The spectrum of the sawtooth waveform is shown in Fig. 6(b).

The repetition rate tunability is also evaluated. To do so, the microwave frequency is continuously increased from 2 to 4 GHz while maintaining the other parameters in the system unchanged. A sawtooth waveform with an increased repetition rate is generated. Fig. 6(c) and (e) shows the sawtooth waveforms at 3 and 4 GHz and the corresponding spectra are shown in Fig. 6(d) and (f). The RMSEs of the experimentally generated sawtooth waveforms are also calculated. For the sawtooth waveforms at 2, 3, and 4 GHz, the RMSEs are 0.1160, 0.1158, and 0.1158, respectively, showing small deterioration as compared with the theoretical RMSE of 0.1156 for the sawtooth waveform with three Fourier series components. Again, the small deterioration is due to the difference between the theoretical and experimental power distributions of the Fourier series components.

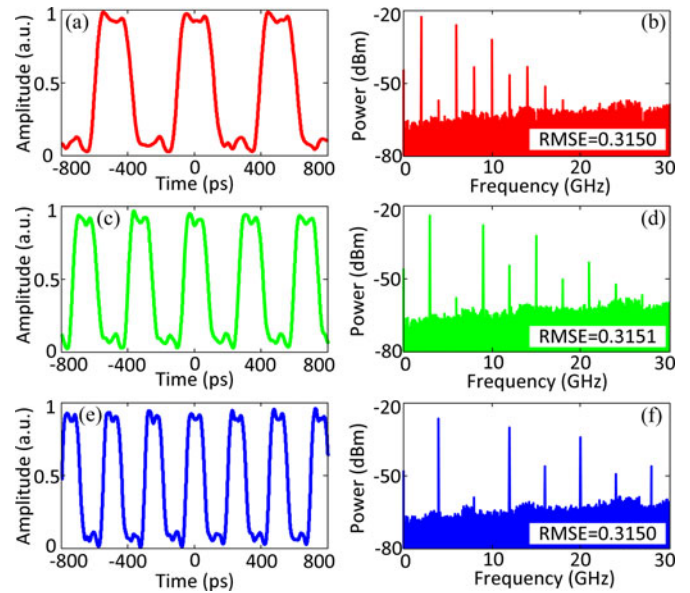


Fig. 7. Experiment results. (a) Generated square waveform with a repetition rate of 2 GHz, and (b) its spectrum. (c) Generated square waveform with a repetition rate of 3 GHz, and (d) its spectrum. (e) Generated square waveform with a repetition rate of 4 GHz, and (f) its spectrum.

### C. Square Waveform

To generate a square waveform, the power of the microwave signal is controlled to be 26 dBm, corresponding to a modulation index of 6.10. By tuning PC2 and PC3, the second-order sidebands are suppressed. The non-modulated optical signal is combined with the modulated signal at the PBS. By applying the optical signal to the high speed PD, a square waveform with a repetition rate identical to the frequency of the reference microwave signal is generated. In the experiment, when the microwave frequency is tuned at 2 GHz, a sawtooth waveform with a repetition rate of 2 GHz is generated, as shown in Fig. 7(a). The spectrum of the sawtooth waveform is shown in Fig. 7(b).

Again, the repetition rate tunability is evaluated by continuously increasing the modulated microwave frequency from 2 to 4 GHz while maintaining the other parameters in the system unchanged. Fig. 7(c) and (e) shows the square waveforms at 3 and 4 GHz and the corresponding spectra are shown in Fig. 7(d) and (f). The RMSEs of the experimentally generated square waveforms are also calculated. For the square waveforms at 2, 3, and 4 GHz, the RMSEs are 0.3150, 0.3151, and 0.3150, respectively. The theoretical RMSE calculated in the simulation for the square waveform with two Fourier series components is 0.3147. Again, the experimentally generated waveforms match well with the theoretical waveforms.

## IV. DISCUSSION AND CONCLUSION

The key significance of the proposed approach is the frequency-independent repetition rate tuning, a feature that is important for applications where the repetition rate is required to be tunable. In the experiment, the repetition rate was tuned from 2 to 4 GHz for the three types of waveforms. The tunable range could be increased if an electrical amplifier with a higher

output over a wider bandwidth is used to amplify the reference sinusoidal microwave signal to drive the PolM. The major limitation of the proposed approach is that the powers of the Fourier series components cannot be tuned individually, which reduces the flexibility of the proposed approach for arbitrary microwave waveform generation.

In summary, we have proposed and experimentally demonstrated a new approach to generating microwave waveforms with a continuously tunable repetition rate using a single PolM in a Sagnac loop. The fundamental concept of the approach is to use the Sagnac loop incorporating the PolM to generate a pulse train with its Fourier series containing the harmonics corresponding to a microwave waveform to be generated. Due to the bi-directional use of the PolM which performs effective modulation for a light wave passing through it along the clockwise direction and no modulation for a light wave along the counter-clockwise direction, and the flexibility to control the polarization states in the loop, microwave waveforms with the required spectrum can be generated. The key significance of the proposed system is the frequency independent repetition rate tuning, which simplifies the generation of microwave waveforms with a large tunable range. In addition, because of the use of a Sagnac loop, in which the two counter propagation light waves were traveling within the same fiber loop, the environmental changes have limited impact on the system stability. The proposed system was theoretically analyzed and experimentally demonstrated. The generation of a triangular waveform, a sawtooth waveform, and a square waveform with a continuously tunable repetition rate from 2 to 4 GHz was demonstrated.

## REFERENCES

- [1] A. W. Rihaczek, *Principles of High-Resolution Radar*. Norwood, MA, USA: Artech House, 1996.
- [2] J. P. Yao, "Photonic generation of microwave arbitrary waveforms," *Opt. Commun.*, vol. 284, no. 15, pp. 3723–3736, Jul. 2011.
- [3] R. S. Bhamber, A. I. Latkin, S. Boscolo, and S. K. Turitsyn, "All-optical TDM to WDM signal conversion and partial regeneration using XPM with triangular pulses," in *Proc. 34th Eur. Conf. Opt. Commun.*, Brussels, Belgium, 2008, pp. 1–2.
- [4] A. I. Latkin, S. Boscolo, R. S. Bhamber, and S. K. Turitsyn, "Optical frequency conversion, pulse compression and signal copying using triangular pulses," in *Proc. 34th Eur. Conf. Opt. Commun.*, Brussels, Belgium, 2008, pp. 1–2.
- [5] F. Parmigiani, M. Ibsen, T. T. Ng, L. A. Provost, P. Petropoulos, and D. J. Richardson, "Efficient optical wavelength conversion using triangular pulses generated using a superstructured fiber Bragg grating," in *Proc. Opt. Fiber Commun. Conf.*, San Diego, CA, USA, 2008, p. OMP3.
- [6] C. B. Huang, D. E. Leaird, and A. M. Weiner, "Time-multiplexed photonically enabled radio-frequency arbitrary waveform generation with 100 ps transitions," *Opt. Lett.*, vol. 32, no. 22, pp. 3242–3244, Nov. 2007.
- [7] J. Ye, L. Yan, W. Pan, B. Luo, X. Zou, A. Yi, and S. Yao, "Photonic generation of triangular-shaped pulses based on frequency to time conversion," *Opt. Lett.*, vol. 36, no. 8, pp. 1458–1460, Apr. 2011.
- [8] H. Wang, A. I. Latkin, S. Boscolo, P. Harper, and S. K. Turitsyn, "Generation of triangular-shaped optical pulses in normally dispersive fibre," *J. Opt.*, vol. 12, no. 3, pp. 035205-1–035205-5, Feb. 2010.
- [9] J. Li, X. Zhang, B. Hraimel, T. Ning, L. Pei, and K. Wu, "Performance analysis of a photonic-assisted periodic triangular-shaped pulses generator," *J. Lightw. Technol.*, vol. 30, no. 11, pp. 1617–1624, Jun. 2012.
- [10] V. Torres-Company, M. Fernández-Alonso, J. Lancis, J. C. Barreiro, and P. Andrés, "Millimeter-wave and microwave signal generation by low-bandwidth electro-optic phase modulation," *Opt. Exp.*, vol. 14, no. 21, pp. 9617–9626, Aug. 2006.

- [11] K. N. Berger, B. Levit, B. Fischer, and J. Azaña, "Picosecond flat-top pulse generation by low-bandwidth electro-optic sinusoidal phase modulation," *Opt. Lett.*, vol. 33, no. 2, pp. 125–127, 2008.
- [12] V. Torres-Company, J. Lancis, P. Andrés, and L. R. Chen, "Reconfigurable RF-waveform generation based on incoherent-filter design," *J. Lightw. Technol.*, vol. 26, no. 15, pp. 2476–2493, Aug. 2008.
- [13] V. Torres-Company and L. R. Chen, "Radio-frequency waveform generator with timemultiplexing capabilities based on multiwavelength pulse compression," *Opt. Exp.*, vol. 17, no. 25, pp. 22553–22565, Nov. 2009.
- [14] H. Chi and J. P. Yao, "Symmetrical waveform generation based on temporal pulse shaping using an amplitude-only modulator," *IEEE Electron. Lett.*, vol. 43, no. 7, pp. 415–417, Mar. 2007.
- [15] W. Liu, L. Gao, and J. P. Yao, "Photonic generation of triangular waveforms based on a polarization modulator in a Sagnac loop," in *Proc. IEEE Int. Top. Meet. Microw. Photon.*, Alexandria, VA, USA, Oct. 28–31, 2013, pp. 68–71.
- [16] J. D. Bull, N. A. F. Jaeger, H. Kato, M. Fairburn, A. Reid, and P. Ghanipour, "40 GHz electro-optic polarization modulator for fiber optic communications systems," *Proc. SPIE*, vol. 5577, pp. 133–143, 2004.
- [17] S. Pan and J. P. Yao, "Optical clock recovery using a polarization-modulator-based frequency-doubling optoelectronic oscillator," *J. Lightw. Technol.*, vol. 27, no. 16, pp. 3531–3539, Aug. 2009.
- [18] W. Liu, M. Wang, and J. P. Yao, "Tunable microwave and sub-terahertz generation based on frequency quadrupling using a single polarization modulator," *J. Lightw. Technol.*, vol. 31, no. 10, pp. 1636–1644, May 2013.

**Weilin Liu** (S'10) received the B.Eng. degree in electronic information engineering from the University of Science and Technology of China, Hefei, China, in 2009, and the M.A.Sc. degree in electrical and computer engineering in the School of Electrical Engineering and Computer Science, University of Ottawa, Ottawa, ON, Canada, in 2011. He is currently working toward the Ph.D. degree in the Microwave Photonics Research Laboratory, School of Electrical Engineering and Computer Science, University of Ottawa, Ottawa, ON, Canada.

His research interests include microwave/terahertz generation, optical signal processing, fiber Bragg grating, and their applications in microwave photonic systems.

**Jianping Yao** (M'99–SM'01–F'12) received the Ph.D. degree in electrical engineering from the Université de Toulon, Toulon, France, in December 1997. He joined the School of Electrical Engineering and Computer Science, University of Ottawa, Ottawa, ON, Canada, as an Assistant Professor in 2001, where he became an Associate Professor in 2003 and a Full Professor in 2006. He was appointed the University Research Chair in Microwave Photonics in 2007. From July 2007 to June 2010, he was the Director of the Ottawa-Carleton Institute for Electrical and Computer Engineering. Prior to joining the University of Ottawa, he was an Assistant Professor in the School of Electrical and Electronic Engineering, Nanyang Technological University, Singapore, from 1999 to 2001.

He has published more than 450 papers, including more than 250 papers in peer-reviewed journals and 190 papers in conference proceedings. He served as a Guest Editor for the Focus Issue on Microwave Photonics in *Optics Express* in 2013. He is currently a Topical Editor for *Optics Letters*, and serves on the Editorial Board of the *IEEE TRANSACTIONS ON MICROWAVE THEORY AND TECHNIQUES*. He is a Chair of numerous international conferences, symposia, and workshops, including the Vice-TPC Chair of the 2007 IEEE Microwave Photonics Conference, TPC Cochair of the 2009 and 2010 Asia-Pacific Microwave Photonics Conferences, TPC Chair of the high-speed and broadband wireless technologies subcommittee of the 2009–2012 IEEE Radio Wireless Symposia, TPC Chair of the microwave photonics subcommittee of the 2009 IEEE Photonics Society Annual Meeting, TPC Chair of the 2010 IEEE Microwave Photonics Conference, and General Cochair of the 2011 IEEE Microwave Photonics Conference. He received the 2005 International Creative Research Award at the University of Ottawa. He received the 2007 George S. Glinski Award for Excellence in Research. He was selected to receive an inaugural OSA outstanding reviewer award in 2012. He serves as an IEEE Distinguished Microwave Lecturer for 2013–2015.

Dr. Yao is a registered Professional Engineer of Ontario. He is a Fellow of the Optical Society of America, and a Fellow of the Canadian Academy of Engineering.